

**3D LASER IMAGING OF IRON METEORITES.** C. Fry<sup>1</sup>, C. Samson<sup>1</sup>, P.J.A. McCausland<sup>2</sup>, and R.K. Herd<sup>1,3</sup>,  
<sup>1</sup>Department of Earth Sciences, Carleton University, Ottawa, Ontario, Canada, K1S 5B6, <sup>2</sup>Department of Earth Sciences, University of Western Ontario, London, Ontario, Canada N6A 5B7, <sup>3</sup>Earth Sciences Sector, Natural Resources Canada, Ottawa, Ontario, Canada K1A 0E8.

**Introduction:** Our group has pioneered the use of laser imaging to build 3D models of meteorites to determine their volume and density<sup>[1,2,3]</sup>. Unlike other methods of volume determination, such as immersion in water or cutting away irregular surfaces, the use of 3D laser imaging is non-destructive and allows and imaged object to be preserved in its current condition. Few density results exist for iron meteorites<sup>[4]</sup>. All meteorites imaged so far have been stony meteorites except for a fragment of the Mundrabilla fragment IAB-ung iron<sup>[2]</sup>. It had an unusual Y shape, leading to difficulty in constructing a 3D model of it from laser images. Mundrabilla gave inconsistent density results ( $7.71 \pm 0.07 \text{ g/cm}^3$  for laser imaging vs  $7.21 \pm 0.31 \text{ g/cm}^3$  for the Archimedean bead method)<sup>[2]</sup>. In this study, several fragments from four different iron meteorites from the National Meteorite Collection of Canada have been imaged for the first time.

**Methods:** A Konica-Minolta Vivid 9i non-contact 3D laser camera was used to image 7 iron meteorite fragments. Fifty-two 3D images of each meteorite fragment were taken at a resolution of 640 by 480 voxels. A turntable was used to rotate the fragments in increments of 20°. After a complete rotation, the sample was flipped to a different rotation axis so that all sides could be imaged. Additional images were taken to capture edges in detail, allowing complete coverage of all fragment surfaces.

After the imaging process was completed, the images were imported into a visualization software, where a human operator assembled them into a closed 3D model (Figure 1B, Figure 2). The edges around each image were trimmed as often they are distorted by field-of-view curvature, causing tiny surficial protrusions on the model. Also eliminated were surfaces which exhibited an unrealistic stretched texture from being imaged at grazing incidence by the laser beam. Following these manual editing steps, the software automatically eliminated redundant data so that the model was covered by a single surface. Finally, the model was edited one last time manually to fill any persistent holes or to remove irregularities.

**Sample selection:** The fragments imaged belong to the Canyon Diablo (IAB-MG), Odessa (IAB-MG), Sikhote-Alin (IIAB) and Toluca (IAB-sLL) iron meteorites. Samples were selected to represent a range of meteorite shapes and surface features, natural or not, to test the capabilities of the laser camera. The meteorites have rounded to angular edges, blocky to flat shapes, and some of the samples

possess cut and etched. The outside of the 67.62g Sikhote-Alin fragment has been cleaned and is bright metallic. The range of surface features imaged included cracks, deep and shallow regmaglypts, smooth and irregular surfaces, variable amounts of rust on the ablation surfaces and usually some combination of these is present.

**Discussion on imaging:** The laser camera readily captured obvious surface features such as regmaglypts or cracks. The Odessa and Toluca samples (Figure 1B, Figure 2A) are seen to have rounded-angular edges, with visible depressions on the surface. The Toluca sample imaged has a cut face, where etching revealed a distinctive cross-hatch (Widmanstätten) pattern formed by the intergrowth of kamacite and taenite. The Vivid 9i camera records cartesian coordinates without intensity information; it was not capable of capturing the full pattern (mostly an intensity feature). Some cross-hatching is visible on the completed model, Figure 2B, indicating that subtle variations in surface roughness associated with the pattern were imaged.

Imaging some metallic surfaces was challenging. Cut faces, were captured easily directly when facing the camera; when at an angle to the camera, they would fail to return signal. Also seen were holes in some images where the dark ablation surface on the sample had worn away revealing metallic iron-nickel underneath. Selecting a slightly different scene from the image bank usually negated this issue. The sample of Sikhote-Alin (67.62g) that had been cleaned was especially difficult to image. A large number of images contained topographic errors in the form of spikes or protrusions. The completed model was covered in these, and needed to be edited extensively.

The camera did not always image sharp edges very well. If an edge comes to a sharp point, there is a distinct possibility that the same small gap will occur in several images. This is exacerbated by the need to trim the edges of each image and to remove areas with a stretched texture. In some cases, both sides of the edge exhibited gaps. It is possible to fill in the holes automatically; however, this approach might lead to an under-representation of the volume of the fragment.

**Density results:** The densities measured by 3D laser imaging range from  $7.46\text{-}7.99 \text{ g/cm}^3$ . As pure nickel-iron has a density of  $7.8 \text{ g/cm}^3$ , it can be

inferred that sulphide or other inclusions are present in the meteorites<sup>[4]</sup>.

The laser imaging method has been shown to produce results consistent with the Archimedeian bead method for stony meteorites<sup>[2]</sup>. The densities of other fragments of the Odessa and Canyon Diablo meteorites have been measured using the Archimedeian bead method by other researchers. Their results were  $7.15 \pm 0.13 \text{ g/cm}^3$  and  $7.38 \pm 0.13 \text{ g/cm}^3$  respectively<sup>[5]</sup>. As for Mundrabilla, there seems to be a bias towards an overestimation of densities by the 3D laser imaging method<sup>[2]</sup>. The 67.62 brushed sample of Sikhote-Alin yielded a questionable, very high density. The density range of the 3 other Sikhote-Alin fragments is more realistic and could indicate a heterogeneous iron mass.

**Future work:** Future work will involve continued use of the 3D laser imaging method to image iron meteorites and measure bulk densities. With an expanding database of results, any systematic bias in density estimations will be better characterized and investigated.

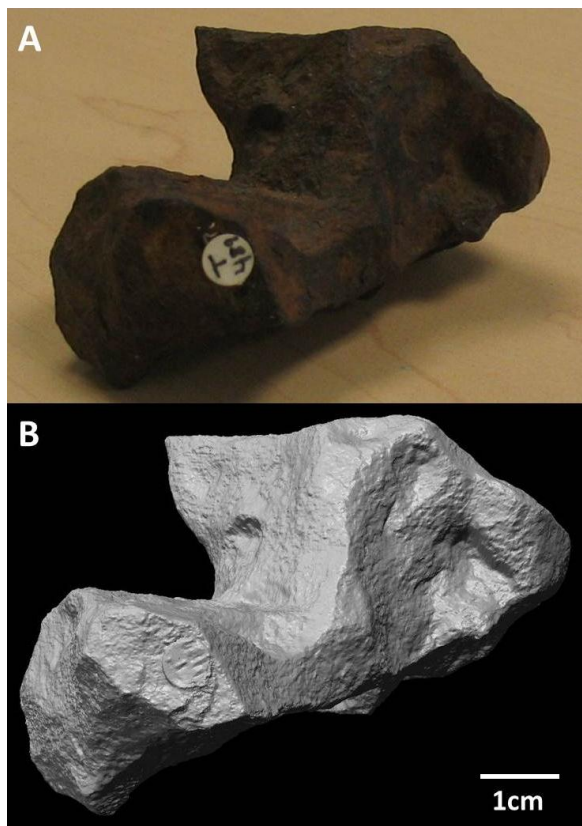


Figure 1: A fragment from the Odessa meteorite. Image A is a digital photo, while image B has been produced using 3D laser imaging. The 3D laser model is a faithful representation of the meteorite and is volumetrically accurate.

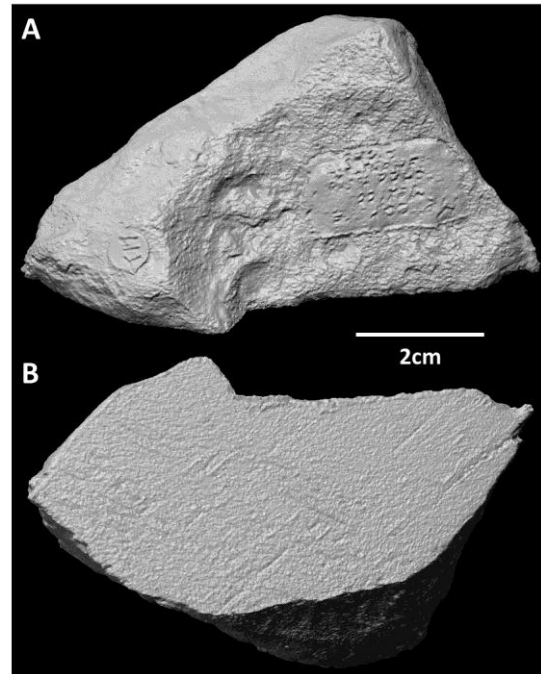


Figure 2: A fragment from the Toluca meteorite, shown in two different orientations. Image A shows the ablation surface of the fragment. A sticker and label that has been painted on can be seen. Image B shows a cut face and also faintly shows crosshatching from mineral intergrowth.

Meteorite	Mass (g)	Volume (cm <sup>3</sup> )	Density (g/cm <sup>3</sup> )
Canyon Diablo	444.75	58.54	7.60
Odessa	396.79	53.51	7.42
Toluca	264.80	35.52	7.46
Sikhote-Alin	68.07	9.04	7.53
Sikhote-Alin	67.62	8.47	7.99
Sikhote-Alin	50.49	7.08	7.69
Sikhote-Alin	50.49	6.50	7.76

Table 1: Bulk volume and density of the meteorite samples studied with 3D laser imaging.

**Acknowledgements:** We thank the Geological Survey of Canada for the loan of the meteorites used in this study.

**References:**[1] Fry, C. et al. (2011) *LPSC XLII*, Abstract #1427. [2] McCausland et al. (2011) *Meteoritics & Planet. Sci.* 46, 1097-1109. [3] Smith D.L. (2006) *JGR*, doi: 10.1029/2005JE00262. [4] Consolmagno, G.J. et al. (2008) *Chemie der Erde*, 68, 1-29. [5] Consolmagno, G.J. and Britt, D.T. (1998) *Meteoritics & Planet. Sci.* 33, 1231-1241.